

On irregularities in the cosmic ray spectrum of $10^{16} - 10^{18}$ eV range.

S. P. Knurenko and I. S. Petrov*

Yu. G. Shafer Institute of Cosmophysical Research and Aeronomy, Yakutsk, Russia
 * igor.petrov@mail.ysn.ru

August 5, 2022



21st International Symposium on Very High Energy Cosmic Ray Interactions (ISVHE-CRI 2022)

Online, 23-27 May 2022

doi:[10.21468/SciPostPhysProc.2](https://doi.org/10.21468/SciPostPhysProc.2)

Abstract

Small, medium and large arrays for the study of cosmic rays of ultra-high energies existing are aimed at obtaining information about our Galaxy and metagalactic space. Concretely search and study of astronomical objects, that forms flux of relativistic particles that fill outer space. The drift and interaction of such particles with magnetic field and shock waves taking place in interstellar space causes the same interest. The shape of the energy spectrum of cosmic rays in the energy range $10^{15} - 10^{18}$ eV, where "knee" and "second knee" is observed, can be formed as a superposition of the partial spectra of various chemical elements. Verification of galactic models, using recent experimental spectral data, makes it possible to study the nature of the galactic and metagalactic components of cosmic rays. The paper presents the result of the energy spectrum of cosmic rays in the range $10^{16} - 10^{18}$ eV measurements obtained at the Small Cherenkov array — a part of the Yakutsk array.

1 Introduction

The study of ultra-high energy cosmic rays has following goals: determination of anisotropy, energy spectrum and mass composition. These are important to advance our understanding of the origin, acceleration and propagation of cosmic rays of different energies. There are different methods for different energy ranges: for energies $10^{12} - 10^{14}$ eV — direct measurements on satellites [1–3] and on balloons [4,5] for energies greater than 10^{14} eV — indirect measurements by extensive air showers method, i.e. by tracking the cascade processes in the atmosphere and detecting charged particles fluxes. Since spectrum of cosmic rays is very wide there are experiments with different sizes: compact ones with an area of $s < 1 \text{ km}^2$ — air showers up to energies of 10^{18} eV, average sized arrays with $s < 20 \text{ km}^2$ — air showers up to energies of 10^{19} eV and huge arrays such as Auger [6], Telescope Array [7] for even greater energies.

2 Small Cherenkov Array

Small Cherenkov array is a part of the Yakutsk array with an area of 1 km^2 and is aimed to register air showers with energies $10^{15} - 10^{18} \text{ eV}$ (Fig. 1). Distinctive feature of the Small Cherenkov is that it measures several components of EAS like muons, electrons and Cherenkov radiation unlike other compact arrays like KASCADE [8] or TUNKA [9]. Such hybrid measurements provide broader outlook at the development of the shower, including longitudinal development, registering the spatial distribution of electrons, muons and EAS Cherenkov light at sea level [10, 11]. Including its longitudinal profile using the measurement of the flux of Cherenkov photons by Cherenkov tracking detectors [11, 12].

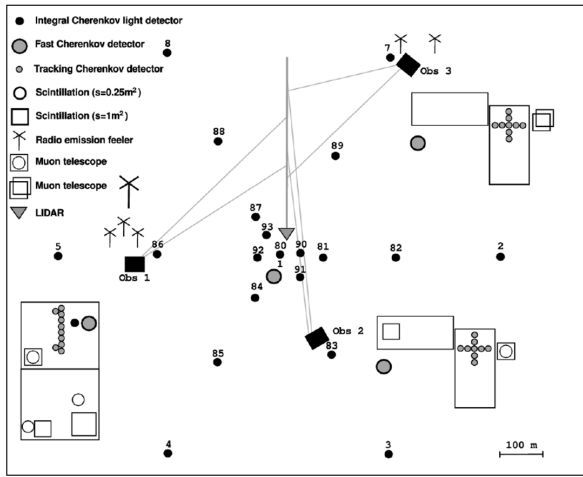


Figure 1: The layout of the detectors of charged particles, muons, and Cherenkov light on the Small Cherenkov array located in the center of the Yakutsk array [13]

3 Air Shower Measurement Simulation at the Small Cherenkov Array

The measurement precision was determined by full Monte Carlo simulation. The precision of air shower characteristics is shown in Table 1.

Measurements is also affected by light loss on aerosol particles in the atmosphere. In addition, transparency of the atmosphere depends on climate, e.g. non-standard atmosphere formed above the Yakutsk array in winter. As shown in the papers [12, 14] near-ground mists and haze during winter can cause significant flux of Cherenkov light attenuation at distances of 100-400 m from the showers axis up to $\sim 30\text{-}40\%$, while under excellent weather conditions losses do not exceed 10%. At the Yakutsk array, the atmosphere is observed regularly [14] and obtained data are taken into account when determining characteristics of air showers, in particular, energy and depth of maximum development [15].

In addition, the simulation algorithm included enumeration of triggers, taking into account detectors threshold, and fluctuations of the threshold in the conditions of background noise while measuring flux of Cherenkov light. Yakutsk array uses two triggers aimed for different energy ranges: $10^{15} - 10^{18} \text{ eV}$ — Small Cherenkov array trigger; $\geq 10^{17} \text{ eV}$ — main trigger from ground scintillation detectors. Fig. 2 shows implementation scheme of the Small Cherenkov array trigger

Table 1: E_0 — air shower energy [PeV]; $\sigma(R)$ — axis reconstruction error [m]; δN_s — total number of charged particles determination error, $\sigma(Q(100))$, $\sigma(Q(200))$ and $\sigma(Q(400))$ — errors of determining the classification parameters of the Cherenkov radiation flux at a distance 100, 200 and 400 m respectively [phot./m²]; $\sigma(\rho_s(300))$ and $\sigma(\rho_s(600))$ — errors of determining of total charged particles flux density at 300 and 600 m respectively [1/m²]; θ — zenith angle determination uncertainty [°]

E_0	$\sigma(R)$	δN_s	$\sigma(Q(100))$	$\sigma(Q(200))$	$\sigma(Q(400))$	$\sigma(\rho_s(300))$	$\sigma(\rho_s(600))$	θ
2	9.7	0.15	0.17	-	-	-	-	1.3
10	7.2	0.11	0.15	-	-	-	-	1.0
100	15.5	0.27	0.15	0.25	-	-	-	1.7
200	14.6	0.32	0.20	0.20	0.22	0.25		1.4
1000	16.7	0.35	-	-	0.20	0.17	0.19	1.3

triangles for air showers with energies of $10^{15} - 10^{18}$ eV

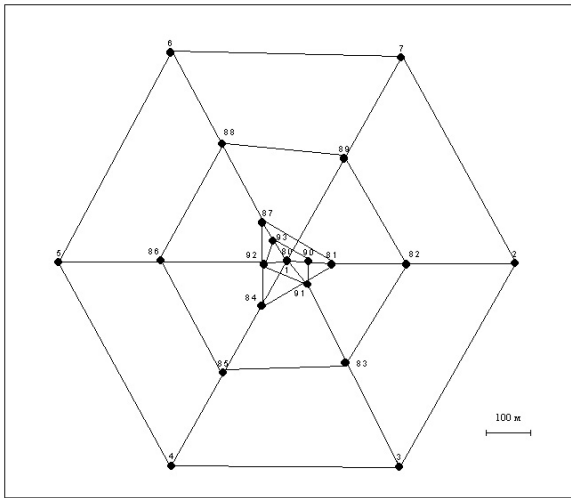


Figure 2: The configuration of trigger triangles used on the Small Cherenkov array [13]

Since different triggers selects air shower events with different energies, there should be transition effect — at the energy threshold boundary, the effective collection area of showers will vary. For large showers, it is underestimated, and for small showers, on the contrary, it is overestimated. With correction of the effective area for events with high-energy showers, this effect is estimated as 15%.

4 Air Shower Energy Estimation

Accuracy for estimation of total number of charged particles at sea level is 10-25%, and for the total flux of Cherenkov light is 10-15% for air showers with an energy $< 5 \cdot 10^{17}$ eV. Such accuracy is good enough to get the necessary information about measured parameters of air showers, for energy estimation by calorimetric method of all air shower components observed at the array: electrons, muons, and the total Cherenkov light flux. The data were obtained at the Small Cherenkov array

for a period 1994 to 2014.

At the Yakutsk array, the primary energy of the particle that produced the air shower is determined by the energy balance method:

$$E_0 = E_{ei} + E_{el} + E_{\mu} + E_{hi} + E_{\mu i} + E_{\nu} \quad (1)$$

The parameters of the formula (1) were determined empirically, for energies in the range $5 \cdot 10^{15} - 3 \cdot 10^{17}$ eV (Table 2). More information about the method can be found in [12].

Table 2: The energy transferred to the different components of the EAS

n/n	lg E _{ei}	lg E _{el}	lg E _μ	lg E _{hi}	lg(E _{mi} +E _ν)	lg E ₀
1	15.687	14.506	14.840	14.465	14.721	15.823
2	15.830	14.612	14.951	14.608	14.832	15.961
3	16.064	14.876	15.175	14.842	15.056	16.195
4	16.345	15.199	15.410	15.123	15.291	16.471
5	16.540	15.362	15.506	15.318	15.387	16.650
6	16.669	15.473	15.644	15.447	15.526	16.783
7	16.797	15.726	15.783	15.575	15.664	16.916
8	16.874	15.851	15.899	15.652	15.780	17.002
9	17.014	16.001	16.015	15.792	15.896	17.139
10	17.116	16.122	16.081	15.894	15.962	17.238
11	17.208	16.269	16.173	15.986	16.054	17.334
12	17.297	16.435	16.306	16.075	16.187	17.436

Energy estimation with parameters Q (100), Q (200) and Q (400) has less uncertainty since of their weak dependence on the zenith angle. We used following formulas to determine these parameters:

$$E_0 = (5.75 \pm 1.39) \cdot 10^{16} \cdot \left(\frac{Q(100)}{10^7} \right)^{0.96 \pm 0.03} \quad (2)$$

$$E_0 = (1.78 \pm 0.44) \cdot 10^{17} \cdot \left(\frac{Q(200)}{10^7} \right)^{1.01 \pm 0.04} \quad (3)$$

$$E_0 = (8.91 \pm 1.96) \cdot 10^{17} \cdot \left(\frac{Q(400)}{10^7} \right)^{1.03 \pm 0.05} \quad (4)$$

where Q (100), Q (200), Q (400) — Cherenkov light flux density at the distances 100, 200 and 400 m respectively.

We can estimate energy scattered in the atmosphere above the observation level by electrons with following equation:

$$E_{ei} = k(x, P_{\lambda}) \cdot \Phi \quad (5)$$

Where Φ is the total flux of Cherenkov light; $k(x, P_{\lambda})$ - approximation coefficient, depends on the transparency of the atmosphere, the nature of the longitudinal development of the shower (energy spectrum of secondary particles and its dependence on the age of the shower) and expressed through X_{max} , measured at the array.

Energy carried below level of observation by electrons

$$E_{el} = 2.2 \cdot 10^6 \cdot N_s(X_0) \cdot \lambda_{eff} \quad (6)$$

where $N_s(X_0)$ is the total number of charged particles at sea level, and λ_{eff} is the absorption range of the shower particles [12].

Fig. 3 shows the dependence of E_{em}/E_0 on energy and comparison of the experimental data with QGSJetII-03 [16] simulations taken from [17]. The parameter E_{em} — is the energy transferred to electromagnetic component of air shower and is equal to $E_{em} = E_{ei} + E_{el}$, and E_0 — total air shower energy.

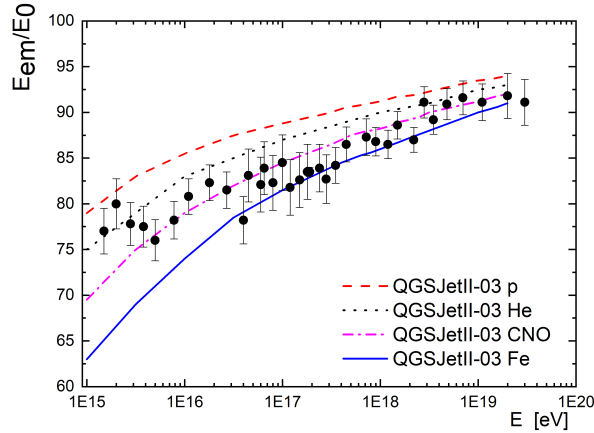


Figure 3: The fraction of energy transferred to the electromagnetic component according to the registration of Cherenkov light of EAS at the Yakutsk array and the QGSJetII-03 model of hadron interactions for the proton p (dash), helium He (dots), CNO nuclei (dash-dot) and iron Fe nucleus (solid).

As can be seen from Fig. 3 on average, the experimental data are consistent with calculations based on the QGSjet-03 model of hadron interactions and the mixed composition of primary particles.

5 Energy spectrum of air showers

Using data of the Small Cherenkov array 1994-2014, we estimated the intensity of air showers in a given intervals in terms of the energy ΔE_i and the zenith angle $\Delta \theta_i$ per unit of the effective area of the array. Fig. 4a shows the resulting spectrum for $10^{15} - 10^{18}$ eV.

As can be seen from Fig. 4a, the obtained spectrum has two features at the energy $\sim 3 \cdot 10^{15}$ eV (first knee) and at the energy $\sim 10^{17}$ eV (second knee). The first knee is characterized by the slope $\gamma_1 = 2.70 \pm 0.03$ and $\gamma_2 = 3.12 \pm 0.03$ and the second knee $\gamma_3 = 2.92 \pm 0.03$ and $\gamma_4 = 3.34 \pm 0.04$.

Fig. 4b shows a comparison with other experiments: TALE [18] TA BR / LR [19], KASCADE-Grande [8] and Tunka [9]. There is a good agreement of the spectra in the energy range $10^{16} - 10^{18}$ eV. All experiments have a break in the spectrum at $\sim 10^{17}$ eV. The discrepancies in the spectrum is partly due to the different methods of energy estimation at various air shower experiments and to some extent by the different effective thresholds of the experiments themselves. Table 3 shows comparison of spectrum slopes between different experiments.

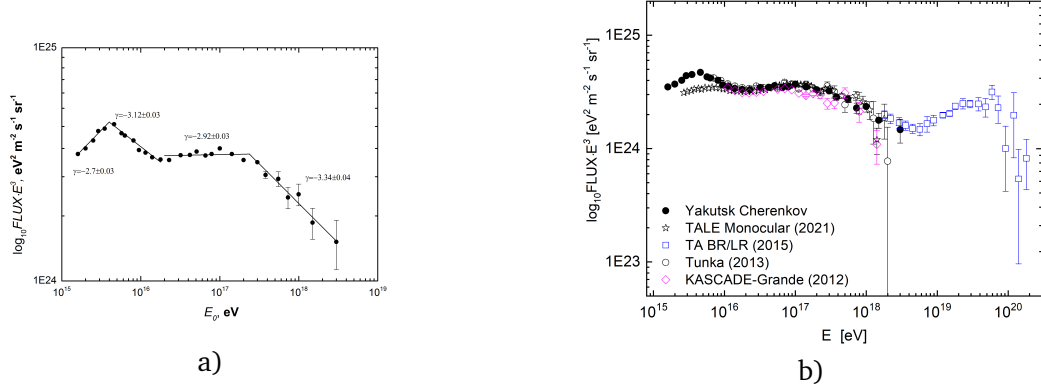


Figure 4: a) A spectrum cosmic ray in the region $10^{16} - 10^{18}$ eV by Yakutsk data [13]; b) Comparison of the spectra of the Yakutsk array (dots), TALE [18] (stars), TA-BR/LR [19], KASCADE-Grande (diamonds) [8] and Tunka (circles) [9]

Table 3: Comparison of the spectrum slopes of different experiments

Energy	Yakutsk	Tunka	KASCADE-Grande	TALE
ΔE , eV	$\gamma \pm \text{stat} \pm \text{sys}$	$\gamma \pm \text{stat} \pm \text{sys}$	$\gamma \pm \text{stat} \pm \text{sys}$	$\gamma \pm \text{stat}$
$(1.2 - 5) \cdot 10^{15}$	$-2.7 \pm 0.04 \pm 0.10$	-	-	-
$(5 - 20) \cdot 10^{15}$	$-3.12 \pm 0.03 \pm 0.07$	$-3.26 \pm 0.01 \pm 0.01$	-	-3.09 ± 0.01
$(2 - 20) \cdot 10^{16}$	$-2.92 \pm 0.03 \pm 0.06$	$-2.98 \pm 0.01 \pm 0.01$	$-2.95 \pm 0.05 \pm 0.02$	-2.89 ± 0.01
$(2 - 30) \cdot 10^{17}$	$-3.24 \pm 0.04 \pm 0.05$	$-3.35 \pm 0.01 \pm 0.01$	$-3.24 \pm 0.08 \pm 0.05$	-3.20 ± 0.02

6 Conclusion

Using a large dataset of Cherenkov light measurements registered for the period of 1994-2014 years, air shower energy is estimated by the energy balance method and the spectrum of cosmic rays in the energy range $10^{16} - 10^{18}$ eV is obtained. At the energy of $\sim 10^{17}$ eV spectrum slope changes from -2.92 to -3.34, which is associated with astrophysical processes in our galaxy, as well as with extragalactic processes. The “second knee” phenomenon can be explained as transition from galactic to extragalactic cosmic rays.

Funding information This work was carried out in the framework of research project No. AAAA-A21-121011990011-8 by the Ministry of Science and Higher Education of the Russian Federation.

References

- [1] O. Adriani, G. C. Barbarino, G. A. Balizevskaya and et al., *PAMELA Measurements of Cosmic-Ray Proton and Helium Spectra*, *Science* **332**, 69 (2011), doi:[10.1126/science.1199172](https://doi.org/10.1126/science.1199172).
- [2] M. Aguilar, D. Aisa, B. Alpat and et al., *Precision Measurement of the Proton Flux in Primary Cosmic Rays from Rigidity 1 GV to 1.8 TV with the Alpha Magnetic Spec-*

trometer on the International Space Station, Phys. Rev. Lett. **114**, 171103 (2015), doi:[10.1103/PhysRevLett.114.171103](https://doi.org/10.1103/PhysRevLett.114.171103).

- [3] D. Green and E. A. Hays, *Measurement of the Cosmic-ray Proton Spectrum with the Fermi Large Area Telescope*, Proc. of Sci. **301**, 159 (2018), doi:[10.22323/1.301.0159](https://doi.org/10.22323/1.301.0159).
- [4] A. Panov, J. A. Jr., H. Ahn and et al., *Energy spectra of abundant nuclei of primary cosmic rays from the data of ATIC-2 experiment: Final results*, Bull. of the RAoS: Physics **73**, 564 (2009), doi:[10.3103/S1062873809050098](https://doi.org/10.3103/S1062873809050098).
- [5] E. Seo, H. Ahn, P. Allison and et al., *CREAM: 70 days of flight from 2 launches in Antarctica*, Adv. Space Res. **42**, 1656 (2008), doi:[10.1016/j.asr.2007.03.056](https://doi.org/10.1016/j.asr.2007.03.056).
- [6] A. Aab, P. Abreu, M. Aglietta and et al., *The Pierre Auger Cosmic Ray Observatory*, NIM A **798**, 172 (2015), doi:[10.1016/j.nima.2015.06.058](https://doi.org/10.1016/j.nima.2015.06.058).
- [7] T. Abu-Zayyad, R. Aida, M. Allen and et al, *The surface detector array of the Telescope Array experiment*, NIM A **689**, 87 (2012), doi:[10.1016/j.nima.2012.05.079](https://doi.org/10.1016/j.nima.2012.05.079).
- [8] W. Apel, J. Arteaga-Velazquez, K. Bekk and et al., *The spectrum of high-energy cosmic rays measured with KASCADE-Grande*, Astropart. Phys. **36**, 183 (2012), doi:[10.1016/j.astropartphys.2012.05.023](https://doi.org/10.1016/j.astropartphys.2012.05.023).
- [9] V. Prosin, S. Berezhnev, N. Budnev and et al., *Tunka-133: Results of 3 year operation*, NIM A **756**, 94 (2014), doi:[10.1016/j.nima.2013.09.018](https://doi.org/10.1016/j.nima.2013.09.018).
- [10] S. Knurenko, V. Kolosov and Z. Petrov, *Cerenkov radiation of cosmic ray extensive air showers. Part 3. Longitudinal development of showers in the energy region of $10^{15} - 10^{17}$ eV*, 27 ICRC (Hamburg) **1**, 157 (2001).
- [11] S. Knurenko, V. Kolosov, Z. Petrov and et al., Sci. and Edu. **4**, 46 (1998).
- [12] S. Knurenko, A. Ivanov, I. Sleptsov and A. Sabourov, *Estimation of the energy of the electron-photon component of cosmic rays on the basis of data for Cherenkov light from ultrahigh-energy extensive air showers*, JETP Lett. **83**, 473 (2006), doi:[10.1134/S0021364006110014](https://doi.org/10.1134/S0021364006110014).
- [13] S. Knurenko, Z. Petrov and I. Petrov, *Second knee on the spectrum of cosmic ray at energies $\sim 10^{17}$ eV by long-termn observations of small cherenkov eas array*, Physics of Atomic Nuclei **82**, 732 (2019), doi:[10.1134/S106377881966027X](https://doi.org/10.1134/S106377881966027X).
- [14] S. Knurenko and I. S. Petrov, *Atmospheric circulation influence during winter on change of air pressure, temperature and spectral transparency at Yakutsk Array*, Proc. SPIE **9292**, 92925B (2014), doi:[10.1117/12.2074877](https://doi.org/10.1117/12.2074877).
- [15] S. Knurenko and I. S. Petrov, *Comparison of the relative transparency of the atmosphere measured by attenuation of Cherenkov light*, Proc. SPIE **10466**, 1046659 (2017), doi:[10.1117/12.2286013](https://doi.org/10.1117/12.2286013).
- [16] S. Ostapchenko, *QGSJET-II: towards reliable description of very high energy hadronic interactions*, Nucl. Phys. B, Proc. Suppl. **151**(1), 143 (2006), doi:[10.1016/j.nuclphysbps.2005.07.026](https://doi.org/10.1016/j.nuclphysbps.2005.07.026).

- [17] R. U. Abbasi, M. Abe, T. Abu-Zayyad and et al., *The Cosmic Ray Energy Spectrum between 2 PeV and 2 EeV Observed with the TALE Detector in Monocular Mode*, ApJ **865**, 74 (2018), doi:[10.3847/1538-4357/aada05](https://doi.org/10.3847/1538-4357/aada05).
- [18] T. Abu-Zayyad, R. Abbasi, M. Allen and et al, *Cosmic ray energy spectrum measured by the tale fluorescence detector*, PoS **395**, 347 (2022), doi:[10.22323/1.395.0347](https://doi.org/10.22323/1.395.0347).
- [19] R. Abbasi, M. Abe, T. Abu-Zayyad and et al, *The energy spectrum of cosmic rays above $10^{17.2}$ eV measured by the fluorescence detectors of the Telescope Array experiment in seven years*, Astropart. Phys. **80**, 131 (2016), doi:[10.1016/j.astropartphys.2016.04.002](https://doi.org/10.1016/j.astropartphys.2016.04.002).